

A Fluorescence-Based Method for Direct Measurement of Submicrosecond Intramolecular Contact Formation in Biopolymers: An Exploratory Study with Polypeptides

Robert R. Hudgins, Fang Huang, Gabriela Gramlich, and Werner M. Nau*

Contribution from the *Departement Chemie, Universität Basel, Klingelbergstrasse 80, CH-4056 Basel, Switzerland*

Received February 22, 2001. Revised Manuscript Received October 26, 2001

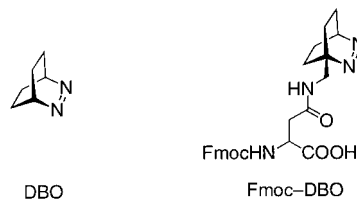
Abstract: A fluorescent amino acid derivative (Fmoc-DBO) has been synthesized, which contains 2,3-diazabicyclo[2.2.2]oct-2-ene (DBO) as a small, hydrophilic fluorophore with an extremely long fluorescence lifetime (325 ns in H₂O and 505 ns in D₂O under air). Polypeptides containing both the DBO residue and an efficient fluorescence quencher allow the measurement of rate constants for intramolecular end-to-end contact formation. Bimolecular quenching experiments indicated that Trp, Cys, Met, and Tyr are efficient quenchers of DBO ($k_q = 20, 5.1, 4.5,$ and $3.6 \times 10^8 \text{ M}^{-1} \text{ s}^{-1}$ in D₂O), while the other amino acids are inefficient. The quenching by Trp, which was selected as an intrinsic quencher, is presumed to involve exciplex-induced deactivation. Flexible, structureless polypeptides, Trp-(Gly-Ser)_n-DBO-NH₂, were prepared by standard solid-phase synthesis, and the rates of contact formation were measured through the intramolecular fluorescence quenching of DBO by Trp with time-correlated single-photon counting, laser flash photolysis, and steady-state fluorometry. Rate constants of 4.1, 6.8, 4.9, 3.1, 2.0, and $1.1 \times 10^7 \text{ s}^{-1}$ for $n = 0, 1, 2, 4, 6,$ and 10 were obtained. Noteworthy was the relatively slow quenching for the shortest peptide ($n = 0$). The kinetic data are in agreement with recent transient absorption studies of triplet probes for related peptides, but the rate constants are significantly larger. In contrast to the flexible structureless Gly-Ser polypeptides, the polyproline Trp-Pro₄-DBO-NH₂ showed insignificant fluorescence quenching, suggesting that a high polypeptide flexibility and the possibility of probe–quencher contact is essential to induce quenching. Advantages of the new fluorescence-based method for measuring contact formation rates in biopolymers include high accuracy, fast time range (100 ps–1 μs), and the possibility to perform measurements in water under air.

Introduction

There is great interest in “intelligent” fluorescent probes for biomolecules that can report information beyond mere detection, e.g., on the structure of polynucleotides and the dynamics of proteins.^{1–6} However, the fluorescence lifetimes of common fluorophores are typically in the range of several nanoseconds or less. This is too short to monitor nanosecond-to-microsecond processes as, for example, the intramolecular contact formation in polypeptides, which is important to understand the functions and folding dynamics of proteins.⁷ To bypass this limitation of fluorescent probes, long-lived triplet-state probes have recently been introduced for measuring the corresponding rates in

polypeptides in the nanosecond-to-microsecond time range by means of transient absorption techniques.^{7–10}

2,3-Diazabicyclo[2.2.2]oct-2-ene (DBO) is a fluorophore with an extremely long fluorescence lifetime (up to 1 μs). As a

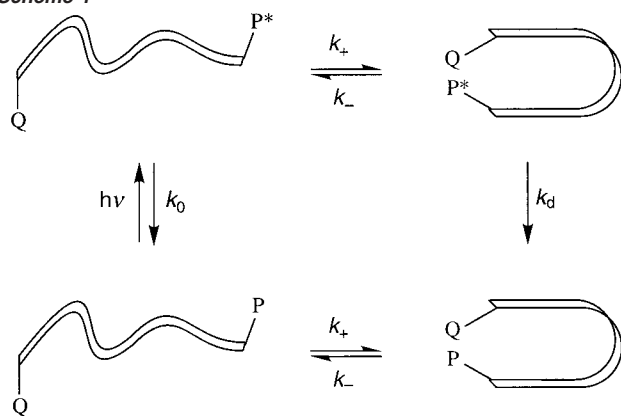


continuation of our efforts to exploit this unique property for uncommon fluorescence-based applications,^{11,12} we employ herein a DBO-labeled fluorescent amino acid, the asparagine derivative Fmoc-DBO, to introduce DBO into polypeptides and to monitor its intramolecular fluorescence quenching by tryptophan.

- (1) Haran, G.; Haas, E.; Szpikowska, B. K.; Mas, M. T. *Proc. Natl. Acad. Sci. U.S.A.* **1992**, *89*, 11764–11768.
- (2) Demchenko, A. P. *Biochim. Biophys. Acta* **1994**, *1209*, 149–164.
- (3) Seidel, C. A. M.; Schultz, A.; Sauer, M. H. M. *J. Phys. Chem.* **1996**, *100*, 5541–5553.
- (4) Muñoz, V.; Thompson, P. A.; Hofrichter, J.; Eaton, W. A. *Nature* **1997**, *390*, 196–199.
- (5) Deniz, A. A.; Dahan, M.; Grunwell, J. R.; Ha, T.; Faulhaber, A. E.; Chemla, D. S.; Weiss, S.; Schultz, P. G. *Proc. Natl. Acad. Sci. U.S.A.* **1999**, *96*, 3670–3675.
- (6) Lakowicz, J. R.; Nair, R.; Piszczek, G.; Gryczynski, I. *Photochem. Photobiol.* **2000**, *71*, 157–161.
- (7) Eaton, W. A.; Muñoz, V.; Hagen, S. J.; Jas, G. S.; Lapidus, L. J.; Henry, E. R.; Hofrichter, J. *Annu. Rev. Biophys. Biomol. Struct.* **2000**, *29*, 327–359.

- (8) McGimpsey, W. G.; Chen, L.; Carraway, R.; Samaniego, W. N. *J. Phys. Chem. A* **1999**, *103*, 6082–6090.
- (9) Bieri, O.; Wirz, J.; Hellrung, B.; Schutkowski, M.; Drewello, M.; Kiefhaber, T. *Proc. Natl. Acad. Sci. U.S.A.* **1999**, *96*, 9597–9601.
- (10) Lapidus, L. J.; Eaton, W. A.; Hofrichter, J. *Proc. Natl. Acad. Sci. U.S.A.* **2000**, *97*, 7220–7225.
- (11) Nau, W. M. *J. Am. Chem. Soc.* **1998**, *120*, 12614–12618.
- (12) Nau, W. M.; Zhang, X. *J. Am. Chem. Soc.* **1999**, *121*, 8022–8032.

Scheme 1

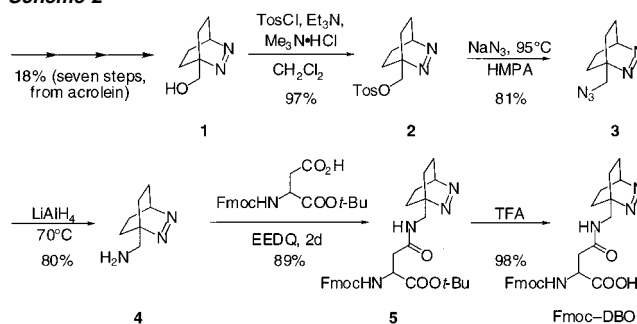


tophan (Trp). This has allowed the first direct measurements of submicrosecond contact formation kinetics in polypeptides by a fluorescence technique.^{13,14}

The general principle behind using photophysical probes to measure peptide dynamics is shown in Scheme 1. A photophysical probe (P) and a quencher (Q) are incorporated into a polypeptide (bottom-left structure). The backbone of the peptide is chosen to behave as a random coil, i.e., without preference for a particular conformation. An excited state of the peptide-bound probe (P*) is prepared with a short light pulse (top-left structure). The dynamics of the polypeptide will infrequently lead to conformations where P* and Q (top-right structure) or P and Q (bottom-right structure) come in contact, and it is this event that is of interest for the evaluation of polymer and biopolymer flexibility. The decay of P*, which can be followed through its characteristic emission or absorption, will reflect the rate of intrinsic excited-state decay (k_0) and the intramolecular quenching rate constant (k_q). Intermolecular quenching is excluded by working at sufficiently low concentrations. If the probe/quencher pair is designed in such a way that molecular contact formation between P* and Q (k_+) is followed by immediate quenching (k_d), k_q equals the pertinent rate of contact formation, k_+ . The condition of “immediate” quenching upon contact is fulfilled when $k_d \gg k_-$, the rate of dissociation of the encounter complex. This criterion is generally assumed to be met when the intermolecular quenching of free P* by free Q in solution occurs near the diffusion-controlled rate. In other cases, k_q will be a function of the three rate constants k_+ , k_- , and k_d , which requires a more involved analysis to extract k_+ , but, on the other hand, may also provide information on k_- .¹⁵

The methodology in Scheme 1 requires a probe with a sufficiently slow intrinsic decay rate, $k_0 \leq k_+$, to allow intramolecular quenching to compete with the natural decay and, thus, to report kinetic information on contact formation. DBO

Scheme 2



is a unique fluorophore due to its long intrinsic fluorescence lifetime (τ_0), which amounts to 325 ns in aerated H₂O, 420 ns in deaerated H₂O, 505 ns in aerated D₂O, and 730 ns in deaerated D₂O.^{12,16} Since $k_0 = 1/\tau_0 = 2.0 \times 10^6 \text{ s}^{-1}$ in aerated D₂O, diffusional processes in the submicrosecond range ($> 10^6 \text{ s}^{-1}$) become accessible.

Experimental Section

Materials. All commercial materials were from Fluka or Aldrich except for Fmoc-Asp-Ot-Bu (Bachem). They were used as received except for HMPA, which was dried (CaH₂) and freshly distilled prior to use, and Me₃N·HCl, which was sublimed in the presence of KOH (0.03 Torr, 100 °C). Column chromatography was performed with silica gel 60–200 μm . The synthetic sequence for Fmoc-DBO in 10% overall yield is shown in Scheme 2. 1-Hydroxymethyl-2,3-diazabicyclo[2.2.2]oct-2-ene (**1**) was synthesized according to a literature procedure¹⁷ and converted to the new 1-aminomethyl-2,3-diazabicyclo[2.2.2]oct-2-ene (**4**) by tosylation, azide substitution, and subsequent reduction with lithium aluminum hydride.

Synthesis of 1-(Aminomethyl)-2,3-diazabicyclo[2.2.2]oct-2-ene (4). For tosylation, the pyridine-free method of Tanabe was used.¹⁸ A solution of *p*-toluenesulfonyl chloride (12.4 g, 65 mmol) in 50 mL of dry CH₂Cl₂ was added to a stirred solution of 1-(hydroxymethyl)-2,3-diazabicyclo[2.2.2]oct-2-ene (5.29 g, 37.7 mmol), Et₃N (6.5 mL, 46.6 mmol), and dry Me₃N·HCl (4.35 mg, 45.5 mmol) in 150 mL of CH₂Cl₂, and the mixture was stirred under nitrogen for 18 h. The mixture was charged with 8.5 mL of *N,N*-dimethylethanolamine, stirred for 10 min, and, after addition of water, was extracted with ethyl acetate. The combined organic layers were washed with water and brine, dried over Na₂SO₄, and concentrated by rotary evaporation to give the sulfonate ester **2** as colorless crystals (10.8 g, 36.6 mmol, 97% yield). Recrystallization from ether afforded colorless needles with mp 119–121 °C: UV (*n*-hexane) λ_{max} 381 nm, ϵ 120 M⁻¹ cm⁻¹; ¹H NMR (400 MHz CDCl₃) δ 1.09–1.15 (2 H, m, CH₂), 1.29–1.35 (2 H, m, CH₂), 1.59–1.64 (4 H, m, CH₂), 2.46 (3 H, s, CH₃), 4.56 (2 H, s, CH₂O), 5.16 (1 H, s br, CH), 7.37 (2 H, d, $J = 8 \text{ Hz}$, CH) 7.86 (2 H, d, $J = 8 \text{ Hz}$, CH) ppm; ¹³C NMR (126 MHz CDCl₃) δ 21.2 (2 C, CH₂), 21.7 (CH₃), 23.2 (2 C, CH₂), 61.7 (CH), 65.6 (C_q), 74.2 (CH₂O), 128.1 (2 C, CH), 129.9 (2C, CH), 132.6 (C_q), 145.0 (C_q) ppm. Anal. Calcd for C₁₄H₁₈N₂O₃S: C, 57.12; H, 6.16; N, 9.52; O, 16.31. Found: C, 57.04; H, 6.21; N, 9.65; O, 16.42.

The sulfonate ester **2** (356 mg, 1.21 mmol) and 400 mg (6.15 mmol) of NaN₃ were dissolved in 10 mL of dry HMPA. The stirred mixture was heated under argon for 14 h at 90 °C (reflux condenser). After cooling, the mixture was diluted with 20 mL of water and extracted four times with ether. The combined extracts were rotary evaporated, redissolved in 25 mL of ether, and washed with 50 mL of water. Drying

(13) Lakowicz, J. R. *Principles of fluorescence spectroscopy*; Plenum Press: New York, 1983.

(14) Waggoner, A. S. In *Applications of fluorescence in the biomedical sciences*; Taylor, D. L., Waggoner, A. S., Lanni, F., Murphy, R. F., Birge, R. R., Eds.; Alan R. Liss, Inc.: New York, 1986; pp 3–28.

(15) It should be noted that the methodology in Scheme 1 is subject to two additional assumptions. First it is assumed that the diffusion rate constants in the excited-state resemble those in the ground state (top and bottom equilibria in Scheme 1). This assumption may be fulfilled for the association rate (k_+) but will not generally apply for the dissociation rate (k_-) due to the possibility of excited-state binding (exciplexes and excimers). Further, it is assumed that the rate constants are not governed by the diffusive behavior of the probe and the quencher (e.g., due to hydrophobe association) to allow an extrapolation to a characteristic dynamic property of the peptide backbone.

(16) Nau, W. M.; Greiner, G.; Rau, H.; Wall, J.; Olivucci, M.; Scaiano, J. C. *J. Phys. Chem. A* **1999**, *103*, 1579–1584.

(17) Engel, P. S.; Horsey, D. W.; Scholz, J. N.; Karatsu, T.; Kitamura, A. *J. Phys. Chem.* **1992**, *96*, 7524–7535.

(18) Yoshida, Y.; Sakakura, Y.; Aso, N.; Okada, S.; Tanabe, Y. *Tetrahedron* **1999**, *55*, 2183–2192.

over MgSO₄ and rotary evaporation gave the azide **3** (170 mg crude product, 81%) with ~5% HMPA. This intermediate was not purified for the next step due to its instability even at low temperature: ¹H NMR (400 MHz, CDCl₃) δ 1.15–1.25 (2 H, m, CH₂), 1.32–1.43 (2 H, m, CH₂), 1.51–1.68 (4 H, m, CH₂), 3.90 (2 H, s, CH₂–N₃), 5.17 (1 H, s br, CH); ¹³C NMR (101 MHz, CDCl₃) δ 21.7 (2 C, CH₂), 24.2 (2 C, CH₂), 58.3 (CH₂–N₃), 61.9 (CH), 67.0 (C_q) ppm.

A solution of azide **3** (164 mg, 0.99 mmol) in 10 mL of dry THF was added dropwise to a stirred slurry of lithium aluminum hydride (76 mg, 2 mmol) in THF (5 mL) under nitrogen. The mixture was stirred at 68 °C for 6 h, cooled to room temperature, diluted with 10 mL THF, and slowly treated with 15% NaOH until a white, granular precipitate was formed. The precipitate was removed by filtration and washed with THF, and the combined filtrates were evaporated. The residue was dissolved in CH₂Cl₂ and dried over KOH pellets. Concentration and flash column chromatography (CH₂Cl₂/methanol/NEt₃ 89:10:1) gave the amine **4** (111 mg, 80%) as a colorless, hygroscopic wax melting at room temperature: UV (D₂O) λ_{max} 369 nm, ε 43 M⁻¹ cm⁻¹ (D₂O); ¹H NMR (400 MHz, CDCl₃) δ 1.18–1.25 (2 H, m, CH₂), 1.31–1.48 (4 H, m, CH₂), 1.60–1.67 (2 H, m, CH₂), 1.78 (2H, br s, NH₂), 3.21 (2 H, br s, CH₂N), 5.14–5.17 (1 H, m, CH) ppm; ¹³C NMR (101 MHz, CDCl₃) δ 22.0 (2 C, CH₂), 24.0 (2 C, CH₂), 49.2 (1 C, CH₂N), 61.9 (1 C, CH), 67.2 (1 C, C_q) ppm. The hygroscopic nature of the pure amine prevented an accurate elemental analysis.

Synthesis of Fmoc-DBO. Amine **4** (80 mg, 0.575 mmol), Fmoc-Asp-Or-Bu (240 mg, 0.583 mmol) and 184 mg of EEDQ (0.75 mmol) were stirred in 15 mL of dry CH₂Cl₂ under argon for 2 days. The mixture was diluted to 50 mL, washed successively with 5% citric acid, water, saturated NaHCO₃, water, and brine, and dried over MgSO₄. Concentration and flash column chromatography (CH₂Cl₂ with 2% MeOH) gave the amide **5** (272 mg, 89%) as a colorless solid with mp 178–180 °C: ¹H NMR (CDCl₃, 500 MHz) δ 1.06–1.16 (2 H, m, CH₂), 1.24–1.35 (2 H, m, CH₂), 1.47 (9 H, s, CH₃), 1.45–1.66 (4 H, m, CH₂), 2.78 (1 H, dd, *J* = 16.0, 4.4 Hz, β-CH₂ Asp), 2.95 (1 H, dd, *J* = 16.0, 4.4 Hz, β-CH₂ Asp), 3.82 (2 H, d, *J* = 6.1 Hz, CH₂N), 4.21 (1 H, t, *J* = 7.4 Hz, CH Fmoc), 4.28 (1 H, dd, *J* = 10.4, 7.4 Hz, CH₂ Fmoc), 4.39 (1 H, dd, *J* = 10.4, 7.4 Hz, CH₂ Fmoc), 4.48–4.52 (1 H, m, α-CH Asp), 5.20 (1 H, br s, CH), 6.05 (1 H, br d, *J* = 8.5 Hz, urethane NH), 6.55 (1 H, br t, *J* = 6.1 Hz, NH), 7.30 (2 H, t, *J* = 7.4 Hz, CH Fmoc), 7.40 (2 H, t, *J* = 7.4 Hz, CH Fmoc), 7.58–7.62 (2 H, m, CH Fmoc), 7.76 (2 H, d, *J* = 7.4 Hz, CH Fmoc) ppm; ¹³C NMR (CDCl₃, 126 MHz) δ 21.7 (2 C, CH₂), 24.1 (2 C, CH₂), 27.9 (3 C, CH₃), 38.0 (CH₂ Asp), 45.3 (CH₂N), 47.1 (CH Fmoc), 51.3 (CH Asp), 62.0 (CH), 66.8 (C_q), 67.2 (CH₂ Fmoc), 82.3 (C_q), 119.9 (2 C, CH Fmoc), 125.2 (2 C, CH Fmoc), 127.0 (2 C, CH Fmoc), 127.7 (2 C, CH Fmoc), 141.3 (2 C, C_q Fmoc), 143.8 (C_q Fmoc), 143.9 (C_q Fmoc), 156.1 (C=O Fmoc), 170.0 (C=O), 170.3 (C=O); FAB⁺ MS (NBA) 533 (M + H⁺), 571 (M + K⁺). Anal. Calcd for C₃₀H₃₆N₄O₅·0.2CH₂Cl₂: C, 66.00; H, 6.68; N, 10.19; O, 14.55. Found: C, 65.81; H, 6.82; N, 10.10; O, 14.42.

Amide **5** (181 mg, 0.340 mmol) in 5 mL of dry CH₂Cl₂ was converted to the free carboxylic acid by adding 3 mL of TFA to the ice-cooled solution and subsequent stirring at room temperature for 3 h. Rotary evaporation of the mixture and coevaporation with toluene and acetonitrile gave Fmoc-DBO (160 mg, 98%) as a colorless solid, which was used directly for peptide synthesis: ¹H NMR (CDCl₃, 500 MHz) δ 1.07–1.19 (2 H, m, CH₂), 1.26–1.39 (2 H, m, CH₂), 1.50–1.57 (2 H, m, CH₂), 1.61–1.68 (2 H, m, CH₂), 2.81 (1 H, dd, *J* = 15.6, 8.1 Hz, β-CH₂ Asp), 3.03 (1 H, dd, *J* = 15.6, 2.7 Hz, β-CH₂ Asp), 3.74–3.88 (2 H, m, CH₂N), 4.20 (1 H, t, *J* = 7.2 Hz, CH Fmoc), 4.30–4.40 (2 H, m, CH₂ Fmoc), 4.52–4.57 (1 H, m, α-CH Asp), 5.20 (1 H, br s, CH), 6.23 (1 H, br d, *J* = 4.7 Hz, urethane NH), 7.30 (2 H, t, *J* = 7.5 Hz, CH Fmoc), 7.39 (2 H, t, *J* = 7.5 Hz, CH Fmoc), 7.44 (1 H, br t, *J* = 11 Hz, NH), 7.56–7.60 (2 H, m, CH Fmoc), 7.75 (2 H, d, *J* = 7.5 Hz, CH Fmoc); ¹³C NMR (CDCl₃, 126 MHz) δ 21.7 (2 C, CH₂), 24.2 (CH₂), 24.3 (CH₂), 37.8 (CH₂ Asp), 45.7 (CH₂N), 47.0 (CH

Fmoc), 50.6 (CH Asp), 62.2 (CH), 67.2 (C_q), 67.3 (CH₂ Fmoc), 120.0 (2 C, CH Fmoc), 125.2 (2 C, CH Fmoc), 127.1 (2 C, CH Fmoc), 127.7 (2 C, CH Fmoc), 141.3 (2 C, C_q Fmoc), 143.8 (2 C, C_q Fmoc), 156.0 (C=O Fmoc), 172.1 (C=O), 172.6 (COOH); FAB⁺ MS (NBA) 477 (M + H⁺); 515 (M + K⁺). HR-MS: calcd 477.2137 (M + H⁺); found (+ESI-TOF) 477.2120.

Peptide Synthesis. Polypeptides were made by Affina Immuntechnik GmbH (Berlin, Germany). The raw polypeptide was precipitated in diethyl ether and purified by semipreparative HPLC (LC-8A, Shimadzu) on an RP-18 column at 40 °C (VYDAC No. 218TP101522, 10 μL). Flow rates of 0.7 (250 × 4.5 column) or 8 mL min⁻¹ (250 × 22 column) with water containing 0.1% trifluoroacetic or phosphoric acid as eluent were adjusted to which a gradient of up to 50% acetonitrile containing 0.1% trifluoroacetic or phosphoric acid as coeluent was applied within 20 min. The retention times ranged between 10 and 22 min. The purity of the polypeptides was >95% as determined by MALDI-MS and HPLC. UV spectrophotometry confirmed also the presence of the characteristic chromophores (DBO, Trp). The extinction coefficients were the same, within error, as those reported for Trp (~5500 M⁻¹ cm⁻¹)¹⁹ and DBO (50 M⁻¹ cm⁻¹),^{12,20} which provides another purity and sample identity criterion.

The DBO probe and the Fmoc-DBO amino acid are fully compatible with standard Fmoc solid-phase peptide synthesis. No complications were found in coupling, and there was no apparent degradation of DBO during cleavage with 95% trifluoroacetic acid and HPLC purification. No special scavengers²¹ or protecting groups are required for the DBO residue during synthesis and cleavage.

Fluorescence Spectroscopy. All measurements were performed in aerated D₂O at ambient temperature. Fluorescence lifetimes were measured on a laser flash photolysis (LFP) setup (LP900, Edinburgh Instruments, Edinburgh, Scotland) with 7-mJ, 355-nm pulses of 4-ns width from a Nd:YAG laser (Minilite II, Continuum, Santa Clara, CA), and with a time-correlated single-photon counting (SPC) fluorometer (FLS900, Edinburgh Instruments) using a 1.5-ns pulse-width H₂ flash lamp at 370 nm. The FLS900 instrument was also used for the steady-state fluorescence (SSF) spectra (λ_{exc} = 365 nm). Fluorescence was detected at 430 nm on both time-resolved setups. The resulting data were analyzed with the Edinburgh software of the LP900 and FLS900 setup by means of monoexponential or biexponential decay functions and a reconvolution function for the excitation light pulse. Intermolecular quenching experiments were performed with 10 μM solutions of DBO and varying quencher concentrations up to 50% quenching effect or up to the solubility limit of the quencher (4–5 data points). Typical concentrations of polypeptides were 10 μM for LFP and 100 μM for SPC experiments. The polypeptides were measured over a concentration range of 1 μM–1 mM by LFP and 10 μM–1 mM by SPC. The fluorescence lifetimes remained constant within error within this concentration range. In the case of SSF measurements, a linear increase of the intensity with concentration (200 μM–1 mM, 5 data points) was found.

Results

Quenching by Amino Acids and Denaturing Agents. The photophysical methodology outlined in Scheme 1 required the selection of a quencher for the excited DBO with an efficient, preferably diffusion-controlled, quenching rate constant. It was appealing to select a natural amino acid as an intrinsic quencher.¹⁰ For this purpose, the quenching rate constants of the parent DBO by the 20 natural amino acids were measured in D₂O, H₂O, and pH 7.0 phosphate buffer. Table 1 reports the data for six amino acids that gave rise to significant quenching

(19) Luisi, P. L.; Rizzo, V.; Lorenzi, G. P.; Straub, B.; Suter, U.; Guarnaccia, R. *Biopolymers* **1975**, *14*, 2347–2362.

(20) Nau, W. M. *EPA Newsl.* **2000**, *70*, 6–29.

(21) Guy, C. A.; Fields, G. B. *Methods Enzymol.* **1997**, *289*, 67–83.

Table 1. Fluorescence Quenching Rate Constants for Natural Amino Acids

amino acid	$k_q/(10^9 \text{ M}^{-1} \text{ s}^{-1})^{a,b}$
tryptophan (Trp)	20
cysteine (Cys)	5.1 [1.5] ^b
methionine (Met)	4.5
tyrosine (Tyr)	3.6 [1.6] ^b
phenylalanine (Phe)	0.08
histidine (His)	0.06

^a Quenching rate constant measured for the parent DBO in D₂O; error in data is 5%. For the remaining 14 naturally occurring amino acids, k_q is less than $1 \times 10^6 \text{ M}^{-1} \text{ s}^{-1}$. ^b Deuterium isotope effects, i.e., $k_q(\text{H}_2\text{O})/k_q(\text{D}_2\text{O})$, are given in brackets for cases where significant effects were observed.

effects. The remaining 14 amino acids quenched at insignificant rates below $1 \times 10^6 \text{ M}^{-1} \text{ s}^{-1}$. The backbone of model polypeptides should be composed of such “inert” amino acids to avoid competitive intramolecular quenching in the actual kinetic measurements of peptide dynamics. The quenching experiments yielded identical results, within error, in buffered (pH 7.0) and unbuffered H₂O, except for quenching by histidine ($\text{p}K_a \sim 6-7$),²² for which the rate increased to $0.76 \times 10^8 \text{ M}^{-1} \text{ s}^{-1}$ in buffer. This indicates that the unprotonated imidazole group is a stronger quencher. Significant solvent isotope effects were observed for Tyr and Cys.

The fluorescence lifetimes of DBO in polypeptides consisting of the above-mentioned “inert” amino acids, i.e., without intramolecular quenchers, were measured for two representative sequences, Gln-Ile-Phe-Val-Lys-DBO-NH₂ and Thr-Leu-Thr-Gly-Lys-DBO-NH₂. The experimental lifetimes in aerated D₂O (510 and 490 ns) were the same, within error, as that of the parent chromophore (505 ns), which confirms the absence of intramolecular quenching by these amino acids in polypeptides.

Only for the four amino acids Trp, Cys, Tyr, and Met did the quenching approach the diffusion-controlled limit with values above $3 \times 10^8 \text{ M}^{-1} \text{ s}^{-1}$. Among these strongest quenchers, Trp and Tyr appear preferable for the design of intramolecular quenching experiments since the two sulfur-containing amino acids Cys and Met have a well-known lability during synthesis and photolysis. Presently, Trp was selected as the most efficient quencher.

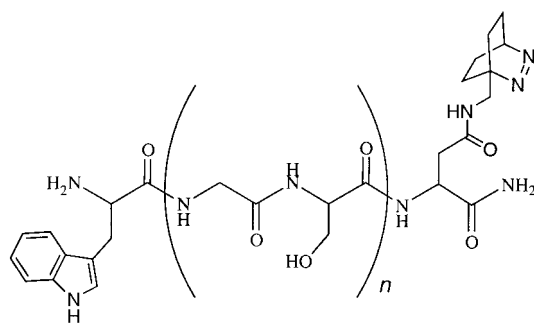
Fluorescence quenching by the denaturing agents urea and guanidinium chloride was found to be insignificant (<10%) up to 5.5 M concentration, with apparent quenching rate constants below $3 \times 10^4 \text{ M}^{-1} \text{ s}^{-1}$. This finding and the fact that the fluorescence lifetime of DBO is insensitive to pH between 2 and 12 should allow for a broad range of experimental conditions for studying peptide dynamics, albeit these have not been exploited in the present study.

Quenching Mechanism. Based on detailed investigations of the fluorescence quenching of the parent fluorophore,^{16,20,23-28}

two viable quenching mechanisms need to be taken into account: hydrogen abstraction^{16,24,25} and exciplex-induced quenching.²⁶⁻²⁸ Both mechanisms require a close probe/quencher contact. The deuterium isotope effect for Tyr and Cys (Table 1) provides evidence that a hydrogen atom abstraction (from the phenolic O–H or the S–H group) is indeed involved, which has in fact been previously observed in the quenching of DBO by the phenol group in α -tocopherol.¹¹ For cysteine, hydrogen abstraction is further supported by the quenching rate constants of methionine (Table 1) and cystine, i.e., the S–S oxidized cysteine dimer ($2 \times 10^8 \text{ M}^{-1} \text{ s}^{-1}$, in D₂O, this work). Although they are both better electron donors than cysteine, they are somewhat less efficient quenchers since they lack the reactive S–H bond.

For tryptophan, no deuterium isotope effect is observed. Moreover, we have evidence from quenching of DBO by dihydroxyindoles²⁹ that hydrogen abstraction from the labile N–H indole bond is inefficient. Hence, the quenching of DBO by Trp is likely to occur through an exciplex intermediate with close contact.²⁶⁻²⁸ This is corroborated by the observation that 1-methyl-Trp, which lacks the N–H bond, is quenched at a very similar rate ($1.6 \times 10^9 \text{ M}^{-1} \text{ s}^{-1}$, in D₂O, this work) as Trp itself ($2.0 \times 10^9 \text{ M}^{-1} \text{ s}^{-1}$). Since exciplexes of n,π^* -excited states, including ketones and azoalkanes, are nonemissive,^{26,30} only indirect evidence for their involvement has been obtained. For the interaction of n,π^* -excited states (which includes DBO) with aromatic donors, the structure of the exciplexes is presumed to involve a singly occupied lone pair orbital of the excited state to face the aromatic π system.³⁰ For amines as electron donors, exciplex formation with DBO is a diffusion-controlled reaction and radiationless deactivation of the exciplex is triggered by a close-lying conical intersection.²⁸ We presume a similar quenching mechanism for singlet-excited DBO by Trp.

Trp-(Gly-Ser)_n-DBO-NH₂ Polypeptides. To establish the overall suitability of the fluorescence-based method for measuring contact formation in biopolymers, we have performed an exploratory study on the length dependence of the intramolecular quenching rate constants between DBO and Trp in structureless peptides. Aerated D₂O was selected for the polypeptide studies, which presents a good tradeoff between the requirement of a long fluorescence lifetime (cf. Introduction), convenient measurement under air, and direct comparison with D₂O NMR data, which are employed in other cases to test for structural effects.



The sequences were chosen to be the (Gly-Ser)_n pairs introduced by Bieri et al., which are supposed to be “structure-

- (22) Abeles, R. H.; Frey, P. A.; Jencks, W. P. *Biochemistry*; Jones and Bartlett Publishers: Boston, 1992.
- (23) Nau, W. M.; Pischel, U. *Angew. Chem., Int. Ed. Engl.* **1999**, *38*, 2885–2888.
- (24) Nau, W. M.; Greiner, G.; Wall, J.; Rau, H.; Olivucci, M.; Robb, M. A. *Angew. Chem., Int. Ed. Engl.* **1998**, *37*, 98–101.
- (25) Nau, W. M.; Greiner, G.; Rau, H.; Olivucci, M.; Robb, M. A. *Ber. Bunsen-Ges. Phys. Chem.* **1998**, *102*, 486–492.
- (26) Pischel, U.; Zhang, X.; Hellrung, B.; Haselbach, E.; Muller, P.-A.; Nau, W. M. *J. Am. Chem. Soc.* **2000**, *122*, 2027–2034.
- (27) Pischel, U.; Allonas, X.; Nau, W. M. *J. Inf. Recording* **2000**, *25*, 311–321.
- (28) Sinicropi, A.; Pischel, U.; Basosi, R.; Nau, W. M.; Olivucci, M. *Angew. Chem., Int. Ed.* **2000**, *39*, 4582–4586.

- (29) Zhang, X.; Erb, C.; Flammer, J.; Nau, W. M. *Photochem. Photobiol.* **2000**, *71*, 524–533.
- (30) Wagner, P. J.; Truman, R. J.; Puchalski, A. E.; Wake, R. *J. Am. Chem. Soc.* **1986**, *108*, 7727–7738.

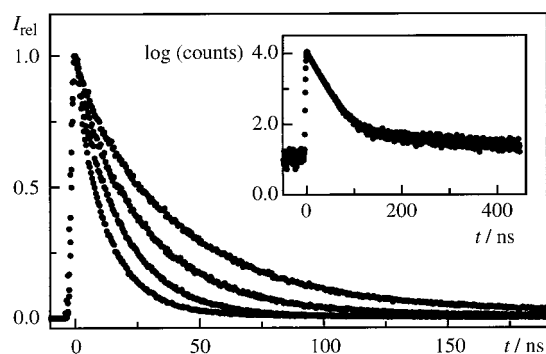


Figure 1. Fluorescence decays (SPC, normalized intensity) of 50 μM aerated D_2O solutions of $\text{Trp}-(\text{Gly-Ser})_n\text{-DBO-NH}_2$ polypeptides ($n = 1, 2, 4, 6$), linear scale. The lowest trace corresponds to $n = 1$, the uppermost one to $n = 6$. Shown in the inset is the decay for $n = 1$ on a semilogarithmic scale; note the long-lived component (1% preexponential factor contribution), which is assigned to a trace impurity.

less⁹. Shown in Figure 1 are the SPC results for the $\text{Trp}-(\text{Gly-Ser})_n\text{-DBO-NH}_2$ polypeptides with $n = 1, 2, 4$, and 6 (structure above). The shortest homologue of the series with $n = 0$, i.e., Trp-DBO-NH_2 , and a longer one with $n = 10$ were also measured. The Poissonian noise statistics of the digital SPC method allows an unsurpassed detection accuracy of minute deviations from monoexponential decay kinetics. As an example, the decay trace for $n = 1$ is shown on a semilogarithmic scale in the inset of Figure 1, which is the preferred SPC data representation mode. Clearly, a second longer lived exponential component is detected, which, however, contributes merely 1% to the total signal intensity (ratio of preexponential factors). This feature may well be due to an impurity. Within the purity specifications of the polypeptides (>95%), the SPC data (and also the LFP data) allow an assignment of monoexponential decay behavior (χ^2 values <1.1). This supports the findings by Bieri et al.⁹ and Lapidus et al.¹⁰ Multiexponential decays have been observed, for example, for fast electron transfer in polypeptides in the picosecond time regime.³¹ As suggested previously,⁹ end-to-end contact formation, which occurs in the nanosecond range, may be sufficiently slow to allow rapid interconversion between the various conformers and, thus, account for the observed monoexponential decay kinetics. A control experiment for a polypeptide with a more rigid, extended polyproline backbone, i.e., $\text{Trp}-(\text{Pro})_4\text{-DBO-NH}_2$, yielded a very long fluorescence lifetime of 460 ns. Monoexponential decay behavior was also observed in this case.

Note that the fluorescence lifetimes of the $\text{Trp}-(\text{Gly-Ser})_n\text{-DBO-NH}_2$ polypeptides range from 10 to 75 ns (Table 2). Fluorescence lifetimes in this region are readily and very accurately measurable by SPC or phase-modulation techniques.¹³ To extract intramolecular quenching rate constants (k_q , Table 2), a correction of the observed lifetimes (τ) for the inherent decay of the excited state (τ_0) according to eq 1 is recommended. The error introduced in k_q by a direct conversion ($k_q \sim 1/\tau$) is small for the present data set (<10%) due to the efficient quenching ($\tau \ll \tau_0$) but cannot generally be neglected. The inherent fluorescence lifetime of the DBO residue in aerated D_2O was taken as 500 ns, which is the average lifetime measured for peptide sequences lacking intramolecular quenchers and for

Table 2. Fluorescence Lifetimes and Intramolecular Quenching Rate Constants for DBO/Trp-Containing Polypeptides^a Obtained from Different Techniques

polypeptide	N^b	τ/ns^c			k_q^d (10^7 s^{-1})
		SPC ^d	LFP ^e	SSF ^f	
$\text{Trp}-(\text{Gly-Ser})_n\text{-DBO-NH}_2$					
$n = 0$	2	23.3	24.5	20	4.1
$n = 1$	4	14.3	13.5	13	6.8
$n = 2$	6	19.5	18.5	18	4.9
$n = 4$	10	30.5	30	29	3.1
$n = 6$	14	45.6	45	[$\equiv 45.6$] ^h	2.0
$n = 10$	22	74.4	76	69	1.1
$\text{Trp-Pro}_4\text{-DBO-NH}_2$	6	460	460	470	<0.02

^a Lifetime of polypeptides not containing Trp or other amino acid quenchers is ~ 500 ns in aerated D_2O , e.g., 510 ns for $\text{Gln-Ile-Phe-Val-Lys-DBO-NH}_2$ and 490 ns for $\text{Thr-Leu-Thr-Gly-Lys-DBO-NH}_2$. ^b Number of peptide units between probe (DBO) and quencher (Trp). ^c Fluorescence lifetime in aerated D_2O at 23 $^\circ\text{C}$. ^d Measured by time-correlated single-photon counting; error in data is 0.3 ns except for $n = 10$ (1.0 ns). ^e Measured by laser flash photolysis; error in data is 5%. ^f Measured by steady-state fluorescence; the slope of the plot of the signal intensity vs the concentration was assumed to be proportional to the lifetime, using the SPC lifetime for $n = 6$ as reference; error in data is 5%. ^g Obtained from eq 1 by using the SPC lifetimes and $\tau_0 = 500$ ns. ^h Reference value.

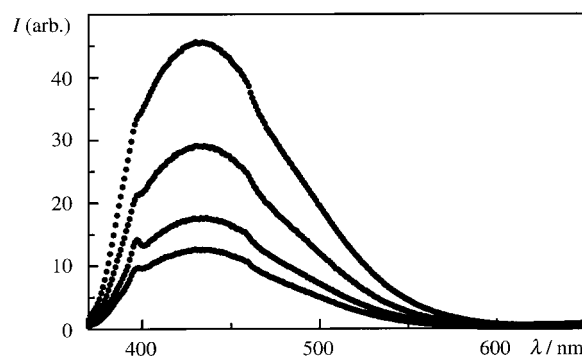


Figure 2. Steady-state fluorescence spectra of 500 μM $\text{Trp}-(\text{Gly-Ser})_n\text{-DBO-NH}_2$ polypeptides ($n = 1, 2, 4, 6$, from bottom to top spectrum) in aerated D_2O . The original intensity (in counts) of each spectrum was divided by the counts in the maximum (430 nm) and multiplied by 45.6, the reference lifetime (in ns) for the $n = 6$ polypeptide (Table 2).

the parent fluorophore. The experimental k_q values are taken as a direct measure of the rate constants for contact formation (k_+); cf. Introduction.

$$k_q = 1/\tau - 1/\tau_0 \approx k_+ \quad (1)$$

The availability of different experimental techniques is a unique advantage of fluorescence measurements^{13,14} and allows for a broad use of fluorescence-based methods in general. Three techniques for measuring fluorescence have been explored: SPC (Figure 1), LFP, and SSF (Figure 2). The mutual agreement that has been obtained by these three methods is excellent (Table 2). While SPC is preferred for high-accuracy results, SSF measurements are more commonly accessible and are well suited for relative lifetime measurements. Note that a reference with a known lifetime is required for the determination of absolute lifetimes by SSF.

Discussion

The purpose of this work is to establish a novel fluorescence-based method for measuring the kinetics of intramolecular contact formation in biopolymers. This requires beforehand a discussion of the advantageous properties of the new fluorophore

(31) G. Jones, I.; Lu, L. N.; Fu, H.; Farahat, C. W.; Oh, C.; Greenfield, S. R.; Gosztola, D. J.; Wasielewski, M. R. *J. Phys. Chem. B* **1999**, *103*, 572–581.

and a comparison with the previously employed techniques, followed by some principal suitability considerations, and, finally, an experimental test with polypeptides of different chain lengths.

Chromophore Characteristics. The distinct photophysical and chemical properties of the parent 2,3-diazabicyclo[2.2.2]-oct-2-ene fluorophore have been discussed previously.^{11,12} For use as a fluorescent label for biomolecules, in particular peptides, certain aspects are particularly noteworthy. First, DBO is small ($\sim 5\text{-\AA}$ diameter) and nearly spherical, which contrasts the established polyaromatic chromophores and luminescent transition metal complexes. Equally important is the high solubility of the neutral parent fluorophore in water, which is related to its high inherent dipole moment of 3.5 D.³² This minimizes the tendency for hydrophobic association^{33,34} and renders the possibility unlikely that the experiment reports on the rate of hydrophobe association³⁵ rather than on the pertinent biopolymer chain mobility.¹⁵ Also, the hydrophilic fluorophore promotes water solubility of the short polypeptides into the millimolar range. This allows standard measurements in water, and a direct comparison with NMR experiments, which are often performed in the same concentration range. The fluorophore has also a high chemical and photochemical stability with decomposition quantum yields of about 0.1% in H₂O³⁶ and 0.3% in D₂O.¹² No change in the fluorescence lifetime was observed even after extended measurements (> 1000 laser pulses) and several days storage in solution.

With respect to the photophysical behavior, the absorption maximum in the near-UV (364 nm)¹¹ and the high fluorescence quantum yield ($\sim 20\%$ in aerated water in the absence of quenchers) are appealing for various instrumental reasons. Common Nd:YAG, XeF excimer and N₂ near-UV laser excitation at 355, 351, and 337 nm can be selected, which by-passes Tyr and Trp excitation and complications due to peptide autofluorescence.¹⁴ The unique property of the parent chromophore, however, is its exceptionally long fluorescence lifetime ($\sim 1\ \mu\text{s}$ in gas phase, 505 ns in aerated D₂O),¹¹ which is the longest among organic chromophores in solution. It is this long fluorescence lifetime that allows the presently described novel kinetic applications and that differentiates this fluorescence-based method from others. It is important to note that the fluorescence of DBO can be monitored under air. This is possible due to the very slow oxygen quenching of DBO in water ($2.1 \times 10^9\ \text{M}^{-1}\ \text{s}^{-1}$) compared to other singlet-excited states.¹²

Techniques for Measuring Submicrosecond Biopolymer Kinetics. Many experiments using chromophore–quencher pairs to measure intramolecular kinetics in *polymers* have been discussed in the literature, including fluorescence quenching and triplet absorption experiments.^{37,38} Related photophysical approaches involve intramolecular excimer formation of pyrene,³³ phosphorescence decay from benzophenone,³⁹ and delayed

fluorescence from triplet–triplet annihilation between anthracene pairs.³⁸ However, few intramolecular quenching experiments have been applied to biomolecules such as peptides.⁷

In the present work, we have employed DBO as a fluorescent probe and Trp as a quencher to measure the rates of intramolecular contact formation in polypeptides. Previous studies on these rates have made use of similar photophysical methodologies but with a different technique (transient triplet absorption) and with different probe/quencher systems,^{8–10} which cannot exploit the advantages of fluorescence as a detection technique.^{13,14} McGimpsey et al. examined two systems with benzophenone as a probe and naphthalene as quencher (Bzp/Nap).⁸ Triplet benzophenone was obtained by a 355-nm laser flash (5-ns pulse width) in deaerated acetonitrile, but intramolecular energy transfer to naphthalene was too fast to allow measurement (< 10 ns). This Bzp/Nap system also offered the possibility of examining by 308-nm photolysis the (backward) Förster resonance energy transfer (FRET) from the singlet-excited Nap to Bzp. Bieri et al. used thioxanthone as probe and naphthalene as quencher (Thx/Nap).⁹ The fast kinetics of contact formation in short polypeptides was quantified for the first time in this study. The Thx triplet was produced by 351-nm laser excitation (20-ns pulse width) in degassed ethanol and in mixtures with water and glycerol. The triplet energy transfer, which in this case was rigorously established through the time-resolved rise of the Nap triplet, occurred near the diffusion-controlled limit, but was reversible and inefficient under some conditions, which precluded studies in water. Lapidus et al. used two natural amino acids, namely, tryptophan as probe and cysteine (and lipoate) as quencher (Trp/Cys).¹⁰ The Trp triplet was populated with 290-nm dye laser pulses (8 ns) in N₂O-saturated water. The quenching rate constant for Cys fell below the diffusion limit, and a correction was introduced by comparison with the more efficient intramolecular quenching by lipoate. It should be mentioned that the chemical and photochemical stability of the triplet probes Thx⁹ and Trp^{10,40} required attention during peptide synthesis and LFP experiments, respectively.

Each of the above-mentioned methods has its strengths and may be preferable to study a specific aspect of biopolymer kinetics. The advantages of the presently introduced fluorescence-based method (DBO/Trp) comprise, most importantly, the ease of experimental monitoring by fluorescence in water under air with high sensitivity and precision.⁴¹

The DBO-based fluorescence technique is particularly well suited to perform measurements in the fast time range (< 500 ns) and to analyze nonexponential decay behavior. Since recent experiments have demonstrated that the contact formation kinetics of the shortest polypeptides are significantly faster (< 10 and 20 ns, respectively)^{8,9} than previously presumed,⁴² and in fact fall into a critical time range,⁴³ it appears essential to have available techniques that allow accurate measurements of these

(32) Harmony, M. D.; Talkington, T. L.; Nandi, R. N. *J. Mol. Struct.* **1984**, *125*, 125–130.

(33) Lee, S.; Winnik, M. A. *Macromolecules* **1997**, *30*, 2633–2641.

(34) Daugherty, D. L.; Gellman, S. H. *J. Am. Chem. Soc.* **1999**, *121*, 4325–4333.

(35) Johnson, G. E. *J. Chem. Phys.* **1975**, *63*, 4047–4053.

(36) Pischel, U.; Nau, W. M. *J. Phys. Org. Chem.* **2000**, *13*, 640–647.

(37) Winnik, M. A. *Chem. Rev.* **1981**, *81*, 491–524.

(38) Horie, K.; Schnabel, W.; Mita, I.; Ushiki, H. *Macromolecules* **1981**, *14*, 1422–1428.

(39) Winnik, M. A. *Acc. Chem. Res.* **1977**, *10*, 173–179.

(40) Mialocq, J. C.; Amouyal, E.; Bernas, A.; Grand, D. *J. Phys. Chem.* **1982**, *86*, 3173–3177.

(41) Unfortunately, the absorbance of DBO is too low to reach the optimum sensitivity of fluorescence measurements (nM range). Nevertheless, the sensitivity of the DBO measurements compares favorably with that employed in the previous triplet transient absorption experiments with strong absorbers; cf. refs 9 and 10. The SPC detection limit could be significantly lowered by replacement of the hydrogen flash lamp by laser excitation.

(42) Hagen, S. J.; Hofrichter, J.; Szabo, A.; Eaton, W. A. *Proc. Natl. Acad. Sci. U.S.A.* **1996**, *93*, 11615–11617.

(43) Callender, R. H.; Dyer, R. B.; Gilmanshin, R.; Woodruff, W. H. *Annu. Rev. Phys. Chem.* **1998**, *49*, 173–202.

fast kinetic processes. Fluorescence detection opens a unique opportunity along this line since it allows measurement down to the picosecond range.¹³ Measurements with triplet probes are subject to instrumental limitations (typical laser pulse widths around 10 ns)^{8,9} and may also be limited by inefficient ($\sim 13\%$ for Trp)⁴⁴ and slow (~ 2.5 ns for both Trp and Thx)^{45,46} intersystem crossing from the initial singlet-excited state to the triplet, as well as concomitant fluorescence (about 10 and 7% for Trp and Thx, respectively),^{45,47} all of which limit the accessible time scale. Conversely, the triplet probes have lifetimes in the microsecond range due to their spin-forbidden decay ($\sim 30\text{--}40$ μs)^{9,10} and should also be applicable to slower kinetic processes. In contrast, the DBO method is restricted to the submicrosecond range as a consequence of the inherent fluorescence decay lifetime (< 1 μs).^{12,16} The different techniques are thus complementary and cover a large dynamic range.

Distance Dependence of Quenching. The methodology in Scheme 1 requires the quenching of the probe to occur (1) rapidly and (2) upon intimate contact with the quencher, resulting in a diffusion-controlled, contact-induced quenching process. With respect to the requirement of molecular contact, the fluorescence quenching of DBO is unique since its fluorescence quenching requires a close, structurally well-defined molecular approach within van der Waals contact ($2\text{--}3$ Å distance) with an efficient hydrogen^{16,24,25} or electron donor.^{26–28} The related quenching mechanisms, hydrogen abstraction and exciplex-induced quenching, are chemically inefficient and have been studied in experimental and theoretical detail.^{16,20,23–28} For comparison, it should be noted that the triplet–triplet energy transfer in the Thx/Nap probe/quencher pair proceeds supposedly through a Dexter mechanism.⁹ Dexter-type energy transfer does not strictly occur upon van der Waals radius contact but decreases exponentially with distance and orbital overlap, such that quenching events may occur within several nanoseconds at separations of $5\text{--}6$ Å.^{48–50} McGimpsey et al. further suggested for their Bzp/Nap polypeptides that superexchange (through-bond) triplet energy transfer may contribute as well.⁸ The quenching mechanism in the Trp/Cys probe/quencher pair has not been discussed in detail.¹⁰

Intramolecular quenching experiments based on FRET or electron transfer (ET) as the quenching mechanism may provide invaluable information on biomolecular structure and dynamics.^{4–6,31,51–53} However, FRET and ET do not require intimate molecular contact and may well occur over larger distances, e.g., through bond by a superexchange mechanism.⁵¹ Hence, the quenching rates may not directly reflect the rates of intrachain contact formation.^{9,54} For example, in the seminal

FRET work by Haas et al. with polypeptides⁵⁵ containing naphthalene as a probe ($\tau_0 \sim 60$ ns) and dansyl as quencher, energy transfer was found to occur over distances of $22\text{--}35$ Å and there is also substantial evidence for long-range electron transfer in polypeptides.^{31,51,56–58} For the DBO/Trp system, FRET is not possible since the singlet excitation energy of Trp ($E^* = 399$ kJ mol⁻¹)⁴⁵ is much higher than that of DBO ($E^* = 328$ kJ mol⁻¹ in water, calculated from $\lambda_{\text{max}} = 364$ nm).^{23,59}

ET as the fluorescence quenching mechanism of DBO by Trp requires more detailed attention, especially since Trp is known as a strong intrinsic electron donor in peptides with an oxidation potential of $\sim 0.80\text{--}0.85$ V vs SCE at neutral pH.^{53,60} However, the very low reduction potential of DBO ($E_{\text{p,red}} = -2.8$ V vs SCE)²³ results in an endergonic energetics for electron transfer ($\Delta G_{\text{ET}} > 20$ kJ mol⁻¹)⁶¹ which cannot account for the observed quenching rate constants in these polypeptides.⁵⁶ It has been proposed that electron-transfer-induced fluorescence quenching of end-labeled probes by a terminal Trp in polypeptides becomes important when the excited-state reduction potential ($E_{\text{red}} + E^*$) exceeds a value of 1.5 V.⁵³ This is by far not fulfilled for the fluorescent probe DBO, since $E_{\text{red}} + E^* \approx 0.6$ V, which points to another quenching mechanism. Moreover, we have recently ruled out ET for several tertiary amines as quenchers although they have even lower oxidation potentials than Trp.²⁶ The combined results are in line with exciplex-induced quenching but speak against ET. This is important for the interpretations since only the former mechanism requires contact between the probe and the quencher and can therefore be directly related to end-to-end intrachain contact formation.

Quenching Rate Constants. The intermolecular quenching rate constants for the probe/quencher pairs should ideally reflect the values that are commonly accepted for diffusion-controlled reactions of small solutes in a particular solvent.⁶² However, quenching rate constants that fall somewhat below the diffusion-controlled limit may well be acceptable, because the dissociation of an *intramolecular* probe/quencher encounter pair (k_- in Scheme 1) has been suggested¹⁰ to be slower than in the case of an *intermolecular* encounter, presumably due to the rigidity of the polypeptide backbone. This may allow a slower-than-diffusion-controlled quenching process to compete more favorably. This circumstance suggests that probe/quencher pairs whose quenching rate constants fall somewhat below the ideal value may still reliably reflect the rate constants for contact formation in a polypeptide. Even in cases where the quenching rate constants fall significantly below the desired limit, e.g.,

(44) Chen, Y.; Liu, B.; Yu, H.-T.; Barkley, M. D. *J. Am. Chem. Soc.* **1996**, *118*, 9271–9278.

(45) Murov, S. L.; Carmichael, I.; Hug, G. L. *Handbook of Photochemistry*; Marcel Dekker: New York, 1993.

(46) Ley, C.; Morlet-Savary, F.; Jacques, P.; Fouassier, J. P. *Chem. Phys.* **2000**, *255*, 335–346.

(47) Dalton, J. C.; Montgomery, F. C. *J. Am. Chem. Soc.* **1974**, *96*, 6230–6232.

(48) Klán, P.; Wagner, P. J. *J. Am. Chem. Soc.* **1998**, *120*, 2198–2199.

(49) Wagner, P. J.; Klán, P. *J. Am. Chem. Soc.* **1998**, *121*, 9626–9635.

(50) Paddon-Row, M. N. In *Stimulating Concepts in Chemistry*; Vögtle, F., Stoddart, J. F., Shibasaki, M., Eds.; Wiley-VCH: Weinheim, 2000; pp 267–291.

(51) Mishra, A. K.; Chandrasekar, R.; Faraggi, M.; Klapper, M. H. *J. Am. Chem. Soc.* **1994**, *116*, 1414–1422.

(52) Williamson, D. A.; Bowler, B. E. *J. Am. Chem. Soc.* **1998**, *120*, 10902–10911.

(53) G. Jones, I.; Lu, L. N.; Vullev, V.; Gosztola, D. J.; Greenfield, S. R.; Wasielewski, M. R. *Bioorg. Med. Chem. Lett.* **1995**, *5*, 2385–2390.

(54) Thomas, D. D.; Carlsen, W. F.; Stryer, L. *Proc. Natl. Acad. Sci. U.S.A.* **1978**, *75*, 5746–5750.

(55) Haas, E.; Katchalski-Katzir, E.; Steinberg, I. Z. *Biopolymers* **1978**, *17*, 11–31.

(56) Faraggi, M.; DeFelippis, M. R.; Klapper, M. H. *J. Am. Chem. Soc.* **1989**, *111*, 5141–5145.

(57) DeFelippis, M. R.; Faraggi, M.; Klapper, M. H. *J. Am. Chem. Soc.* **1991**, *112*, 5640–5642.

(58) Lee, H.; Faraggi, M.; Klapper, M. H. *Biochim. Biophys. Acta* **1992**, *1159*, 286–294.

(59) For DBO, FRET is generally unlikely due to the low oscillator strength ($f \approx 0.001$) of its lowest n, π^* transition.

(60) DeFelippis, M. R.; Murthy, C. P.; Broitman, F.; Weinraub, D.; Faraggi, M.; Klapper, M. H. *J. Phys. Chem.* **1991**, *95*, 3416–3419.

(61) According to Kikuchi, K.; Takahashi, Y.; Katagiri, T.; Niwa, T.; Hoshi, M.; Miyashi, T. *Chem. Phys. Lett.* **1991**, *180*, 403–408, exciplex formation dominates in this endergonic region over electron transfer, which is in line with our suggested quenching mechanism.

(62) Becker, H. G. O.; Böttcher, H.; Dietz, F.; Rehorek, D.; Roewer, G.; Schiller, K.; Timpe, H.-J. *Einführung in die Photochemie*; Deutscher Verlag der Wissenschaften: Berlin, 1991.

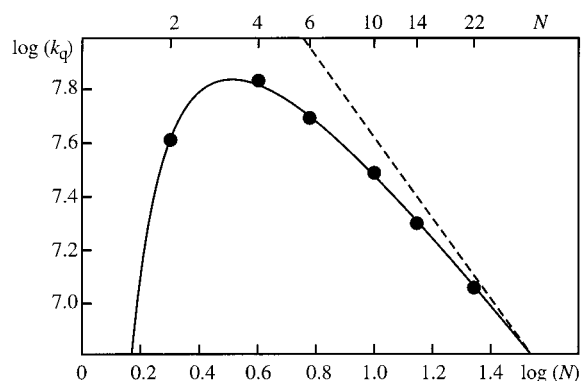


Figure 3. Double-logarithmic plot of the intramolecular quenching rate constant (k_q) of Trp-(Gly-Ser) $_n$ -DBO-NH $_2$ polypeptides vs the peptide length, taken as the number of intervening peptide units (N). The SPC values from Table 2 are used; the statistical errors obtained from this technique result in errors on the same order of magnitude as the size of the data points. A simple function of the type $y = a - 1.5x - b/x$ was fitted to the experimental data ($a = 9.37$ and $b = 0.392$) to reflect the theoretical slope of -1.5 at long chain lengths and the expected rapid falloff (b/x term) at short chain lengths; cf. ref 66. The dashed line has a slope of -1.5 and is shown to illustrate the deviation from the theoretical behavior.

$5.0 \times 10^8 \text{ M}^{-1} \text{ s}^{-1}$ for the Trp/Cys pair in water,^{63,64} the experimental rate data may serve to provide reliable *relative* kinetic data. The absolute rate constants for contact formation, as has been suggested, can be extrapolated.¹⁰

The quenching rate constant for the DBO/Trp pair ($2.0 \times 10^9 \text{ M}^{-1} \text{ s}^{-1}$), like that for the Trp/lipoate pair ($\sim 3 \times 10^9 \text{ M}^{-1} \text{ s}^{-1}$),^{10,63} is close to the diffusion-controlled limit in water ($6.5 \times 10^9 \text{ M}^{-1} \text{ s}^{-1}$),⁶² and the quenching rate of the Thx/Nap pair in ethanol ($4 \times 10^9 \text{ M}^{-1} \text{ s}^{-1}$)⁹ lies close to the diffusion rate constant in ethanol ($5.4 \times 10^9 \text{ M}^{-1} \text{ s}^{-1}$).⁶² These probe/quencher pairs should thus directly report on the rate of intramolecular end-to-end contact formation (k_+ in Scheme 1).

Length Dependence of Polypeptide Contact Formation Rates. To study the length dependence of polypeptide contact formation rates by the intramolecular quenching methodology (Scheme 1), the quencher is generally separated from the probe by a varying number of unreactive amino acids, and it is assumed that the experimental intramolecular quenching rate constants (k_q) are a direct measure of the rate for contact formation (k_+). Previous studies employed transient triplet absorption to study polypeptides with the structures Thx-(Gly-Ser) $_n$ -Nap-Ser-Gly ($n = 1-4$)⁹ and Cys-(Gln-Gly-Ala) $_n$ -Trp ($n = 1-6$).¹⁰ We have now examined the length dependence for Trp-(Gly-Ser) $_n$ -DBO-NH $_2$ polypeptides with $n = 0, 1, 2, 4, 6$, and 10. The DBO residue was attached at the C terminus and Trp was attached as a quencher to the N terminus. Tyrosine or artificial amino acids could be employed instead of tryptophan, but the latter was preferred in view of the fast quenching rate (Table 1) and natural relevance. The fluorescence lifetimes of the polypeptides are entered in Table 2.

The present data are entered in a $\log(k_q)$ - $\log(N)$ plot in Figure 3, where N denotes the number of -CO-NH- peptide units between probe and quencher, i.e., the peptide length.⁶⁵ According to the polymer theory by Flory, which treats the kinetics of

intrachain contact formation within a Gaussian chain approximation, such a plot should be linear with a slope of -1.50 at sufficiently long chain length.^{66,67} A comparison with the same plots provided in the previous studies^{9,10} reveals that the contact formation rates measured with the present fluorescence-based technique (taken as the intramolecular quenching rate constants in Table 2) are significantly and consistently faster at the same length than the previously measured values. The variance from the Thx/Nap data set appears to be quite constant around 40%, while that with the extrapolated Trp/Cys data ranges between 20 and 150%. For example, the rate constants for $N = 4$ and $N = 10$ in the DBO/Trp data set (6.8 and $2.0 \times 10^7 \text{ s}^{-1}$) exceed the results for $N = 3$ and 9 in the Thx/Nap series (5.0 and $1.4 \times 10^7 \text{ s}^{-1}$)⁹ as well as those extrapolated for $N = 4$ and $N = 10$ in the Trp/Cys study (2.7 and $1.7 \times 10^7 \text{ s}^{-1}$).¹⁰ Moreover, the rate constants for $N = 22$ in the DBO/Trp data set, which is the longest polypeptide among those yet studied, is significantly larger than that extrapolated for the shorter $N = 19$ peptide in the Trp/Cys study (11 vs $7.2 \times 10^6 \text{ s}^{-1}$).¹⁰ Whether these variances are due to the selection of different solvents and polypeptide sequences, assumptions related to diffusion-controlled quenching, or structural effects imposed by the probe/quencher pairs cannot be decided at present. However, with respect to the “speed limit”^{7,9,42} for intrachain contact formation in polypeptides, the present data suggest a value as short as 10 ns, which is similar to the upper limit (<10 ns) provided by McGimpsey et al.⁸

That the fluorescence quenching rate constants are indeed a measure of polypeptide chain contacts and not of differential rates of superexchange electron transfer (see above) is evident from the fluorescence lifetime of the shortest homologue of the series ($n = 0$), which is actually higher than those for the two next longer derivatives with $n = 1$ and 2. In addition, the study of a derivative with a polyproline backbone, i.e., Trp-(Pro) $_4$ -DBO-NH $_2$, revealed a much longer fluorescence lifetimes of 460 ns in D $_2$ O, very close to that observed for polypeptides not containing Trp (500 ns). Polyprolines are presumed to have an extended, more rigid structure in solution,^{51,56} such that the longer fluorescence lifetimes can be interpreted in terms of a reduced flexibility of the polyproline backbone, which renders conformations with contact between the probe and the quencher less likely.⁶⁸

It is important to note that the $\log(k_q)$ - $\log(N)$ plot of our data (Figure 3) indicates a pronounced negative curvature with a sharp falloff near $N = 2$. In fact, this sharp falloff is theoretically expected at sufficiently short chain lengths due to the breakdown of the Gaussian chain approximation.⁶⁶ A first indication of a negative curvature for polypeptides was obtained from the Trp/Cys data set.¹⁰ Moreover, if a linear function is fitted through the data for the longer polypeptides with $n =$

(66) Suter, U. W.; Mutter, M.; Flory, P. J. *J. Am. Chem. Soc.* **1976**, *98*, 5740–5745.

(67) Mutter, M.; Suter, U. W.; Flory, P. J. *J. Am. Chem. Soc.* **1976**, *98*, 5745–5748.

(68) The control experiments with both polypeptides also provide additional evidence against superexchange electron transfer as the quenching mechanism (see above). The rate of the latter is expected to increase weakly, but exponentially with the number of peptide units.⁵⁶ If superexchange electron transfer were to play an important role, one would expect a similar quenching rate constant for the Pro and Gly-Ser peptides of the same length and one would expect the fastest rate constant for the shortest dipeptide ($n = 0$). Both are not observed experimentally. It should be noted that the kinetics of intramolecular chain diffusion has actually been an uncertainty in several studies of long-range electron transfer (e.g., refs 51 and 58). The present method should also be of interest in this context.

(63) Bent, D. V.; Hayon, E. *J. Am. Chem. Soc.* **1975**, *97*, 2612–2619.

(64) Gonnelli, M.; Strambini, G. B. *Biochemistry* **1995**, *34*, 13847–13857.

(65) The peptide unit in the asparagine chain (cf. structure) has been counted for the present polypeptides. If it is not counted ($N = 3, 5, 9, 13, 21$), the conclusions with respect to absolute rates, curvature, and slope (-0.91 ± 0.07) remain unchanged.

1–10 (Figure 3, $r^2 = 0.995$), the slope (-1.05 ± 0.06) falls below the theoretical value (-1.50) and the previously reported slope (-1.36 ± 0.26).⁹ While a smaller-than-theoretical slope can again be rationalized in terms of the pertinent approximations,⁶⁶ the contrast in slope between the two experimental studies is interesting in view of the identical polypeptide backbones.

Conclusions

The present fluorescence-based method for measuring sub-microsecond dynamics of polypeptide chain contact formation yields unsurpassed kinetic data with respect to accuracy, detection of nonexponentiality, and time range (100 ps–1 μ s). These features, along with the full compatibility with standard solid-phase peptide synthesis, the high photostability of the small, dipolar probe, and the use in aerated water, are advantageous for a wide range of biological applications. Attachment of the same fluorophore to other biological targets, including

other amino acids and nucleotides, should be viable, which renders the present fluorescence-based method an attractive alternative to assess the kinetics of intramolecular diffusion phenomena in polymers and biopolymers. In particular, this is pertinent for the understanding of protein folding and the domain motions in proteins.

Acknowledgment. R.R.H. thanks the National Science Foundation (U.S.A.) for an International Research Fellowship (grant INT-9901459). This work was generously supported through several grants of the Swiss National Science Foundation (MHV grant 2134-62567.00 for G.G., NF grant 620-58000.99 for W.M.N.). The study was performed within the Swiss National Research Program “Supramolecular Functional Materials” (grant 4047-057552 for W.M.N.). We acknowledge the help of C. Marquez with the Fmoc-DBO synthesis.

JA010493N